

# Experimental Investigations of the UPQC Arrangement

Grzegorz BENYSEK

University of Zielona Gora, Poland

**Summary:** Paper presents the fundamental properties and dependences describing the UPQC (Unified Power Quality Conditioner) arrangements. The UPQC devices simultaneously permit to fulfill the following functions: voltage and current harmonics compensation, network voltage and load current symmetrization as well as network voltage stabilization and power flow control. The selected results of the experimental investigations conducted on the small power laboratory model have been described. Applied method for DC link capacity selection was talked over in details and confirmed with experimental results. Results of experimental investigations, including operation of the UPQC arrangement in case of thyristor rectifier load were also introduced.

**Keywords:**  
power quality,  
power flow control,  
harmonics compensation,  
reactive power  
compensation

## 1. INTRODUCTION

For many years improvement of quality of electric energy delivery, have been one of the most important areas to apply power electronics arrangements. In this area active power filters (APF) occupy significant position [1] and literature in this topic is constantly complemented with new positions [3, 4]. Also another works related to the series-parallel active power filters appeared [2, 10]. Such arrangements, called also “Unified Power Quality Conditioners” [5], continue to be a subject for the intensive investigations. One can connect this with functional possibilities of them, as well as with development of methods and control algorithms. It should be expected, that in short time UPQC arrangements find more and more wide [6, 7], also residential applications [8].

Investigations of the dynamic processes in full model of the UPQC arrangement confirmed small influence of the fast dynamic processes, related to formation of the reference courses, onto considerably slower processes occurring both in DC circuit as well as connected with the reference courses determination [9]. To investigate the slow dynamic processes,

a simplified model is usually good enough. On the base simplified UPQC model, with omission of influence of the fast dynamic processes in LC circuits of the adding sources, method for analytical determination of the DC link capacitance, coupling both parallel and series arrangements, was worked out and verified experimentally. Presented in this paper theoretical investigations are also completed with different experimental results, confirming good filtration-compensating proprieties as well as multi-functionality of the UPQC arrangements.

## 2. INVESTIGATED UPQC

Presented in Figure 1, 3-phase UPQC consists of series (SAPF — Series Active Power Filter) and parallel (PAPF — Parallel Active Power Filter) energetic active filters, joining common DC circuit. SAPF —  $u'_C$  voltage source — filtrates harmonics and stabilizes in point of measurement load voltage  $u_L$ , during source voltage  $u_S$  changes and deformations. PAPF —  $i'_C$  current source — compensates passive

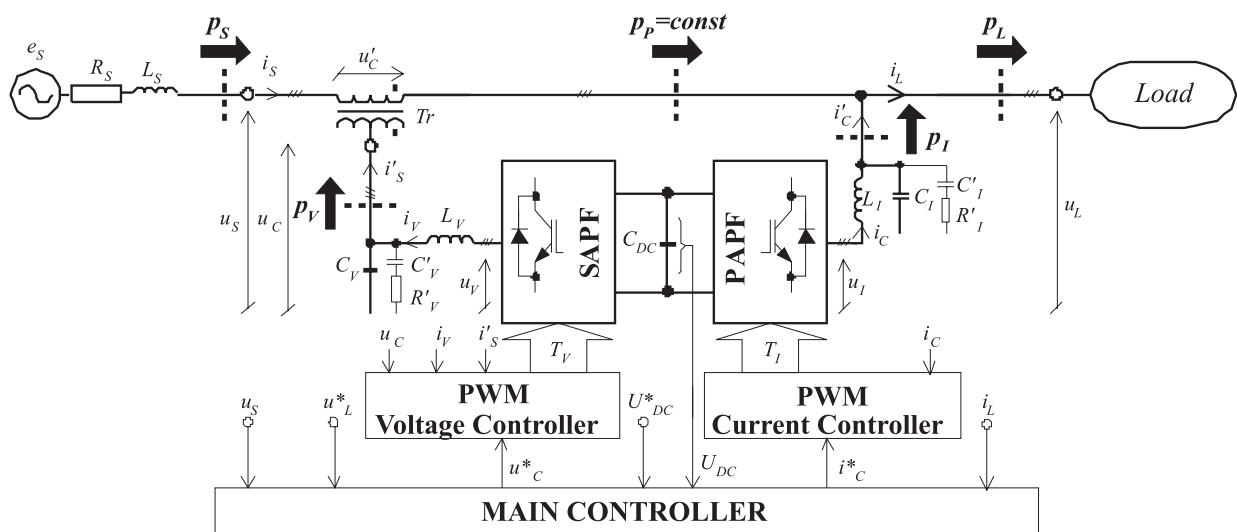


Fig.1. Scheme of the investigated UPQC

components in load current  $i_L$ . Small filters,  $L_V - C_V$  as well as  $L_I - C_I$  (alongside with dumping circuits  $R'_V - C'_V$  as well as  $R'_I - C'_I$ ) provide filtration of the harmonics related to PWM control.

The main controller controls  $U_{DC}$  voltage and on the basis of measured instantaneous values  $i_L, u_S$  as well as reference values  $U^*_{DC}$  and  $u^*_L$ , calculates reference current  $i^*_C$  and voltage  $u^*_C$  courses. Calculations are realized in  $d-q$  coordinates, rotating with frequency  $\omega_S = 2\pi/T_S$ , where:  $T_S$  — period of the network voltage. Unsettling in active power balance:

$$\int_{t-T_S}^t p_V dt = - \int_{t-T_S}^t p_I dt, \quad \int_{t-T_S}^t p_S dt = \int_{t-T_S}^t p_P dt = \int_{t-T_S}^t p_L dt$$

causes  $U_{DC}$  voltage changes. To stabilize this voltage, controller forces additional component, in phase with  $u_I$  voltage, in  $i_C$  current. In  $d-q$  coordinates most often this is a periodic course.

### 3. SLOW PROCESSES IN DC CIRCUIT

To investigate the slow dynamic processes in DC circuit of the UPQC arrangement, usually good enough is simplified model. Such model was introduced in Figure 2. When “ $d-q$ ” coordinates are suitably synchronized with the network voltage, the main controller become very simple. The main controller from principle of operation can exclude the appearance of some current and voltage components in UPQC arrangement. In the case of controller from Figure 2 we always have e.g.:

$$\tilde{i}_{Sd} = 0, \tilde{i}_{Sq} = 0, \bar{i}_{Sq} = 0, \tilde{u}_{Ld} = 0$$

$$\tilde{u}_{Lq} = 0, \bar{u}_{Lq} = 0, \bar{u}_{Sq} = 0$$

where:  $\bar{u}, \bar{i}$  concerns constant and  $\tilde{u}, \tilde{i}$  pulsation components of currents and voltages.

Considering the above, and in accordance with accepted symbols, instantaneous power  $p_{DC}$  delivered to the DC link, can be determined on the basis of the following dependency:

$$p_{DC} = \underbrace{\bar{i}_{Sd} (\bar{u}_{Sd} + \tilde{u}_{Sd} - \bar{u}_{Ld})}_{-p_V} + \underbrace{\bar{u}_{Ld} (\bar{i}_{Sd} - \bar{i}_{Ld} - \tilde{i}_{Ld})}_{-p_I} = \underbrace{(\bar{i}_{Sd} \bar{u}_{Sd} - \bar{u}_{Ld} \bar{i}_{Ld})}_{\Delta P_{\bar{}}} + \underbrace{(\bar{i}_{Sd} \tilde{u}_{Sd} - \tilde{i}_{Ld} \bar{u}_{Ld})}_{\Delta P_{\sim}} \quad (1)$$

The instantaneous active power  $p_{DC}$  is distributed on two components:  $\Delta P_{\bar{}}$  as well as  $\Delta P_{\sim}$ , because of their different influence on changes of  $U_{DC}$  voltage, during steady states as well as transients.

#### 3.1. Steady states

During steady state, component  $\Delta P_{\bar{}} = 0$ , and pulsation frequencies in periodic component  $\Delta P_{\sim}$  depend only on harmonics, network voltage asymmetry and load current.

Let's consider, that  $\Delta P_{\sim}$  component is a superposition of two sinusoidal, with frequency  $\tilde{\omega}_U$  and  $\tilde{\omega}_I$ , courses:

$$\Delta P_{\sim} \approx P_L \left[ K_{SU} \sin(\tilde{\omega}_U t) - K_{LI} \sin(\tilde{\omega}_I t + \varphi_{L/S}) \right] \quad (2)$$

where:

- $\varphi_{L/S}$  — phase shift between courses;
- $K_{SU}, K_{SI}$  — coefficients determining influence of every sinusoidal course on  $\Delta P_{\sim}$  component;
- $P_L$  — average load active power.

In our case:

$$C_{DC} \cdot U_{DC} \frac{dU_{DC}}{dt} = p_{DC} \quad (3)$$

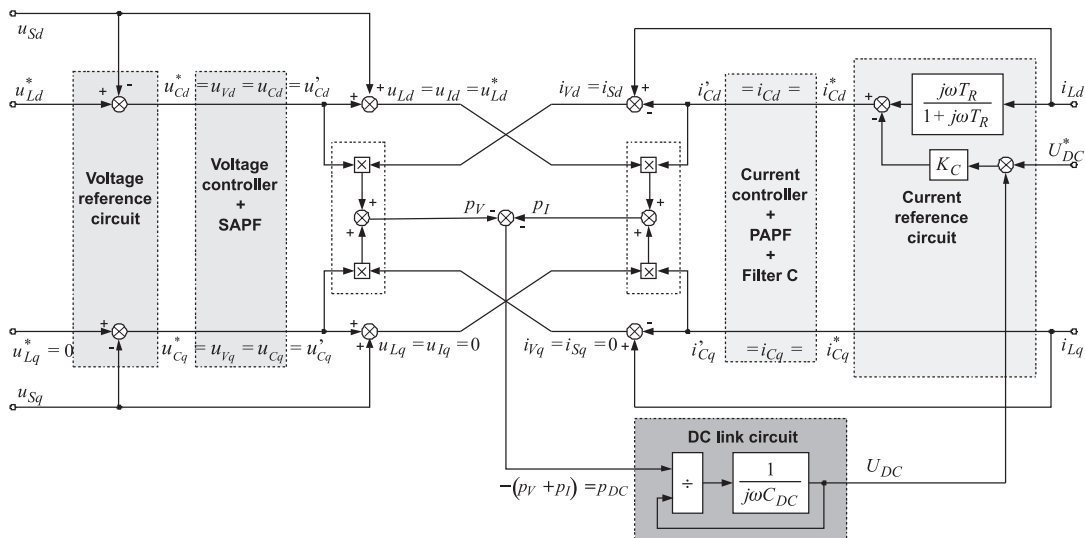


Fig.2. UPQC simplified model, with ideal voltage and current adding sources

and on the base of the following dependencies (1) and (2) we obtain:

$$\frac{C_{DC}}{2} \left[ U_{DC(max)}^2 - U_{DC(min)}^2 \right] \leq 2P_L \left( \frac{K_{SU}}{\tilde{\omega}_U} + \frac{K_{LI}}{\tilde{\omega}_I} \right) \quad (4)$$

where:

$U_{DC(min)}$  — respectively minimum,  
 $U_{DC(max)}$  — maximum,  
 $C_{DC}$  — capacitor voltage.

Taking into consideration that:

$$U_{DC}^* = \left( U_{DC(max)} + U_{DC(min)} \right) / 2$$

and that the  $U_{DC}$  voltage maximum error is:

$$\begin{aligned} \Delta U_{DC(max)} &= U_{DC(max)} - U_{DC}^* = U_{DC}^* - U_{DC(min)} = \\ &= \left( U_{DC(max)} - U_{DC(min)} \right) / 2 \end{aligned}$$

after some algebraic transformations, dependency (4) can be rewritten as:

$$C_{DC} \leq \frac{P_L}{\varepsilon_C U_{DC}^{*2}} \left( \frac{K_{SU}}{\tilde{\omega}_U} + \frac{K_{LI}}{\tilde{\omega}_I} \right) \quad (5)$$

where:

$\varepsilon_C = \Delta U_{DC(max)} / U_{DC}^*$  —  $U_{DC}$  maximum relative error.

$K_{SU}$  and  $K_{SI}$  coefficients, see dependencies (2), (4) and (5) should be quite the same as deformation coefficients of  $u_{sd}$  as well as  $i_{Ld}$  courses:

$$K_{SU} = U_{SD} / U_{SP}, \quad K_{LI} = I_{LD} / I_{LP} \quad (6)$$

where:

$$U_{SP}^2 = \frac{1}{2\pi} \int_0^{2\pi} (\tilde{u}_{sd}(\vartheta))^2 d\vartheta \quad U_{SD}^2 = \frac{1}{2\pi} \int_0^{2\pi} (\tilde{u}_{sd}(\vartheta))^2 d\vartheta$$

$$I_{LP}^2 = \frac{1}{2\pi} \int_0^{2\pi} (\tilde{i}_{Ld})^2 dv \quad I_{LD}^2 = \frac{1}{2\pi} \int_0^{2\pi} (\tilde{i}_{Ld}(\vartheta))^2 d\vartheta$$

$\tilde{\omega}_U$  and  $\tilde{\omega}_I$  are chosen as the lowest frequencies, in components  $\tilde{u}_{sd}$  and  $\tilde{i}_{Ld}$ , spectrum.

$C_{DC}$  capacitor, determined on the base of dependency (5), should be inflated in reference to its value required for correct operation during steady states. Exacter results are given by weighed ratios, considering the full spectra of  $u_{sd}$  and  $i_{Ld}$  courses, although in practice their determination is not required. Mostly  $C_{DC}$  capacitor is determined by the transient states, during load active power step changes and/or network voltage amplitude variations.

### 3.2. Transient states

Let's consider, that in a UPQC (model of which was introduced in Figure 2), load active power step change  $\Delta P_L$  occurred (e.g. additional load was turned on). For constant voltage  $u_{Ld} = \bar{u}_{Ld} = const$  and with higher harmonic omission, this change is identified as load current increase  $\Delta \bar{i}_{Ld} = \Delta P_L / u_{Ld}$ . When the reference current circuit is applied, as it is in Figure 2 [1], changes in compensating current  $i_{Cd}$  are following course:

$$\Delta \bar{i}_{Cd} = \frac{\Delta P_L}{u_{Ld}} e^{-\frac{t}{T_R}} + K_C \cdot \Delta U_{DC} \quad (7)$$

where:

$K_C$  — gain of the  $U_{DC}$  voltage  $P$  regulator

Because  $i_{Ld} = i_{Sd} + i_{Cd}$ , thus changes of compensating currents (7) crate also the network current changes:

$$\Delta \bar{i}_{Sd} = \frac{\Delta P_L}{u_{Ld}} \left( 1 - e^{-\frac{t}{T_R}} \right) - K_C \cdot \Delta U_{DC} \quad (8)$$

Simultaneously with this change, considering (1) and (8), also component  $\Delta P_{\pm}$  in instantaneous power  $p_{DC}$ , is changing:

$$\Delta P_{\pm} = \Delta P_L \cdot (\mu_u - 1) - \mu_u \cdot \Delta P \cdot e^{-\frac{t}{T_R}} - K'_C \cdot \Delta U_{DC} \quad (9)$$

where:

$$\mu_u = u_{sd} / u_{Ld}; \quad K'_C = u_{Ld} \cdot \mu_u \cdot K_C$$

On the base of dependency (3) defining DC link capacitor voltage balance (linearized around  $U_{DC}^*$ ), considering (9) as well as assuming without loss of generality  $\mu_u = 1$ , we have:

$$\Delta U_{DC} = -\frac{\Delta P_L}{K'_C} \cdot \frac{T_R}{(T_R - T_C)} \cdot \left( e^{-\frac{t}{T_R}} - e^{-\frac{t}{T_C}} \right) \quad (10)$$

where:

$$T_C = C_{DC} U_{DC}^* / K'_C$$

On the base of dependency (10) one can say, that voltage  $\Delta U_{DC} = U_{DC} - U_{DC}^*$  changes are function with one extremum, which occurs after time:

$$t_{sup} = T_C T_R \ln T_R / T_C / (T_R - T_C)$$

Putting  $t_{sup}$  to dependency (10) we have:

$$\Delta U_{DC(max)} = -\frac{\Delta P_L}{K'_C} \cdot \left( \frac{T_C}{T_R} \right)^{\frac{T_C}{T_R - T_C}} \quad (11)$$

Considering (10), we have:

$$\left| \Delta U_{DC(max)} \right| < \frac{|\Delta P_L| \cdot T_R}{C_{DC} \cdot U_{DC}^* + K_C' \cdot T_R} \quad (12)$$

Dependency (12) in practical and simple way allows to evaluate influence of the main controller's  $T_R$  and  $K_C$  coefficients, reference  $U_{DC}^*$  voltage,  $C_{DC}$  capacitor and load power  $\Delta P_L$  step changes, on  $U_{DC}$  voltage maximum deviations  $\Delta U_{DC(max)}$ .  $\Delta U_{DC(max)}$  changes, as the function of  $\Delta P_L$  increases, calculated on the base of (12) as well as received experimentally are compared in next chapter.

$C_{DC}$  capacitor, determined on the base of equation:

$$C_{DC} = \frac{T_R}{U_{DC}^*} \cdot \frac{|\Delta P| - K_C' \cdot |\Delta U_{DC(max)}|}{|\Delta U_{DC(max)}|} \quad (13)$$

guarantees, that  $U_{DC}$  voltage will not exceed the acceptable range of changes. Theoretically possible negative  $C_{DC}$  value is result of linearization of equation (2). In practice, from the point of view of required small  $\Delta U_{DC(max)}$  deviations as well as  $K_C'$  limited value, determined with regard of sensor ratio, such negative value is not possible.

At the end,  $C_{DC}$  capacitor should be selected taking into consideration the worst cases, as the largest value from two calculated on the base of equations (5) as well as (13).

#### 4. EXPERIMENTAL RESULTS

In Figure 3, one can see the laboratory setup to investigate the UPQC. In the arrangement, a simple main controller (Figure 2) with type P regulator for voltage  $U_{DC}$  control, was applied. Selected parameters of the laboratory model and adjustments are introduced in Table 1. Further, there are presented results occurred during steady states, transients and showing UPQC power flow control capabilities.

##### 4.1. Steady states results

In Figure 4, the exemplary experimental current and voltage courses, illustrating UPQC steady states filtration capabilities, were introduced. Experimental courses concern situation of an arrangement loaded with controlled 7kW, 6-pulse rectifier ( $\alpha = 0^\circ$ ,  $THD(I_L)$  28%) and supplied with deformed network voltage with distortion coefficient  $THD(U_S)$  9%.

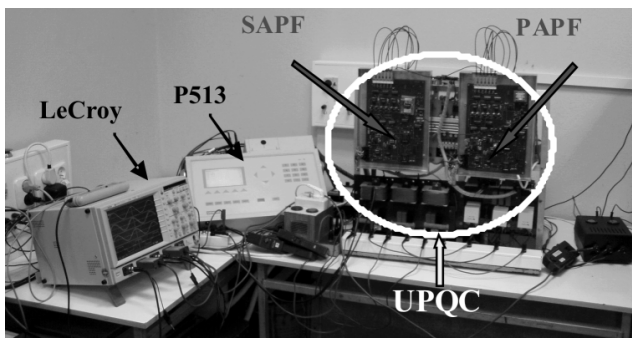


Fig. 3. Experimental model

Table 1. UPQC parameters

Nominal network voltage $U_S$	3×220 V
Admissible range of changes in network voltage	60÷340 V
Stabilized load voltage $U_L$	60÷240 V
DC link capacitor	1650 μF
The reference DC link voltage $U_{DC}^*$	610 V
Maximum network current $I_{S(max)}$	20 A
The main controller, HPF's time constant $T_R$	10 ms
$U_{DC}$ voltage regulator, $K_C$ gain (with assumption of sensor ratio 0,052 V/V)	1 V/V
PWM frequency in <i>PAPF</i> controller	4 kHz
PWM frequency in <i>SAPF</i> controller	12 kHz

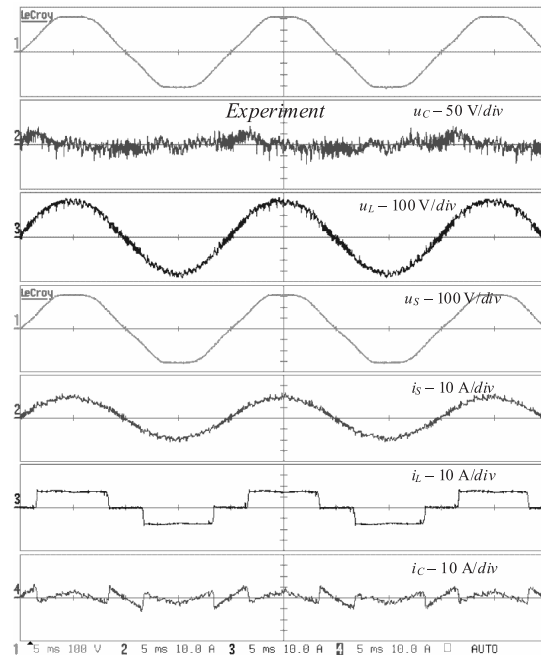


Fig. 4. Experimental courses in situation of network voltage and load current harmonics compensation

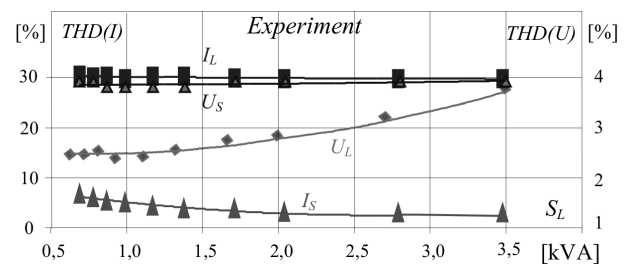


Fig. 5. Current and voltage THD coefficients as a function of load apparent power ( $\alpha = 0^\circ$ )

UPQC filtration proprieties only in slight degree depend on load power (Figure 5). For small loads the  $THD(I_S)$  coefficient increases because of enlarged participation of harmonics, with frequencies related to the PWM triangular carrier in *PAPF* controller. From the other side in case of large loads the  $THD(U_L)$  coefficient increases because of voltage drop on impedance of the adding transformer. This voltage drop is caused by the uncompensated load current harmonics. One should mark, that  $THD(U_L)$  and  $THD(I_S)$  changes show improperly selected  $L_C$  passive filters.

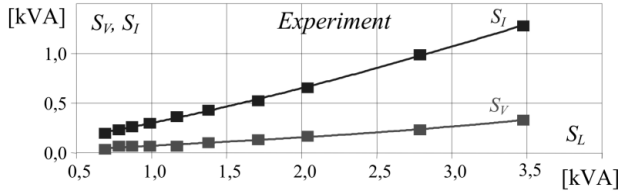


Fig. 6. SAPF ( $S_P$ ) and PAF ( $S_I$ ) nominal powers as a function of load apparent power ( $\alpha = 0^\circ$ )

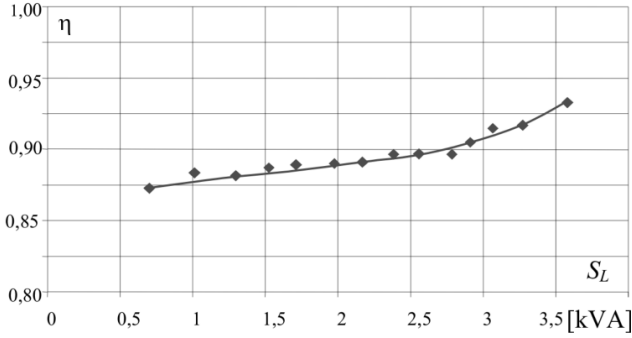


Fig. 7. UPQC efficiency as a function of load apparent power ( $\alpha = 0^\circ$ )

Load changes mainly infect the PAF and SAPF nominal powers (Figure 6). In the general case, PAF nominal power depends on distortion power, reactive power and load asymmetry power, additionally SAPF nominal power depends on active components of the load current, deformations and asymmetry of the network voltage. Experimental dependencies, introduced in Figure 6, concern the case when UPQC is loaded with 6-pulse rectifier and supplied with sinusoidal (THD( $U_S$ ) 4%), symmetrical, nominal voltage.

The nominal powers, however in low degree, depends on SAPF and PAF efficiency. Increasing load power (and network voltage), participation of losses in nominal power decreases. The same dependency concerns in an obvious way, efficiency of the whole UPQC (Figure 7). In case of load apparent power  $S_L = 8,5\text{kVA}$  (not in Figure 7), the measured efficiency was 0,96.

Steady states in the experimental investigations contained also estimation of UPQC potential for load current as well as network voltage symmetrization. Investigations were realized in situation of lowered network (supply) voltage. As the asymmetric load: two, 2-pulse rectifiers, 1,1kVA each, were used. Asymmetric network (supply) voltage was obtained with assistance of three independent autotransformers. Exemplary current and voltage courses are introduced in Figure 8 and Figure 9.

#### 4.2. Transient states results

Experimental verification of dependency (13) was the major aim of investigations held in this chapter. During theoretical calculations the following values were considered:  $T_R = 10\text{ms}$  and  $K_C = 1\text{V/V}$  (see Table 1), nominal network voltage  $U_S = 220\text{V}$ , the reference DC link voltage  $U_{DC}^* = 610\text{V}$ . In laboratory model the  $U_{DC}$  voltage sensor ratio was  $\mu_u = 0,052$ . Allowing the maximum DC link voltage deviation

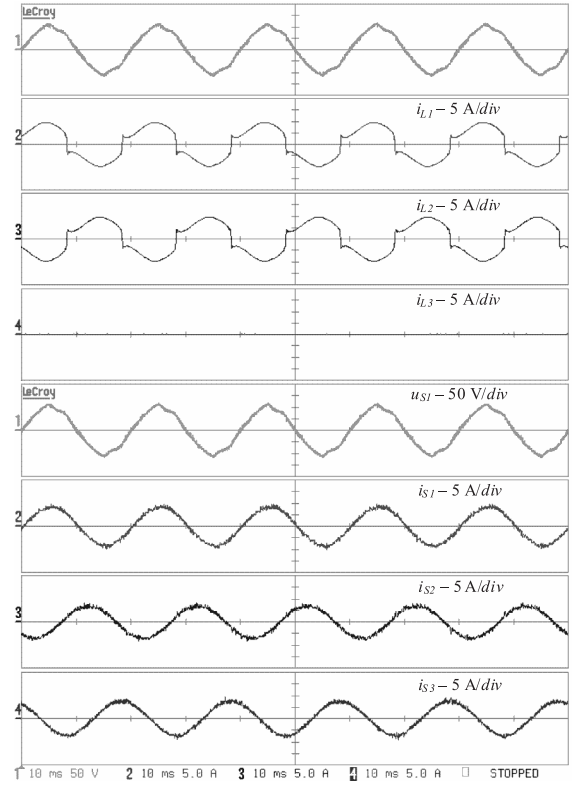


Fig. 8. Experimental courses in situation of symmetrical supply and non-linear and asymmetrical load

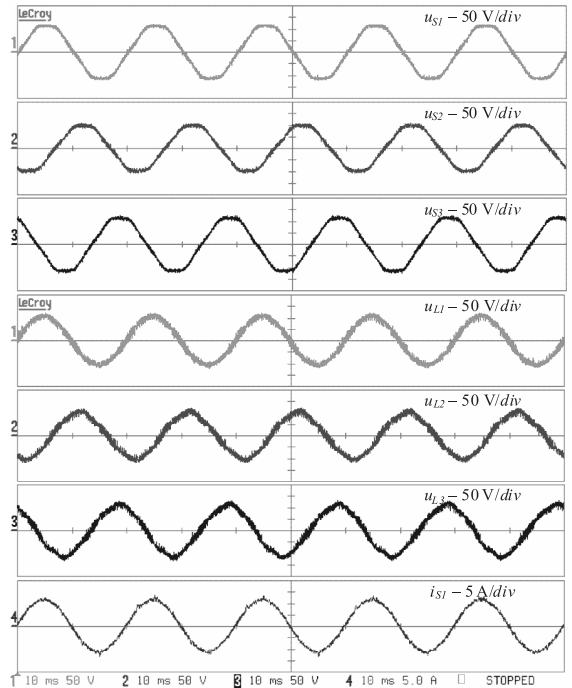


Fig. 9. Experimental courses in situation of asymmetrical supply and symmetrical resistive load.

$\Delta U_{DC(\text{max})} = 30\text{V}$  and load active power step ( $\Delta t = 0$ ) changes  $\Delta P_L < \Delta P_{L(\text{max})} = 4\text{kW}$ , calculated  $C_{DC}$  capacitor totaled  $1850\mu\text{F}$ . In laboratory model, from practical point of view,  $C_{DC} = 1650\mu\text{F}$ , was applied. Results of calculations and experimental investigations, presented in Figure 10 and Figure 11, were obtained for this smaller capacitor.

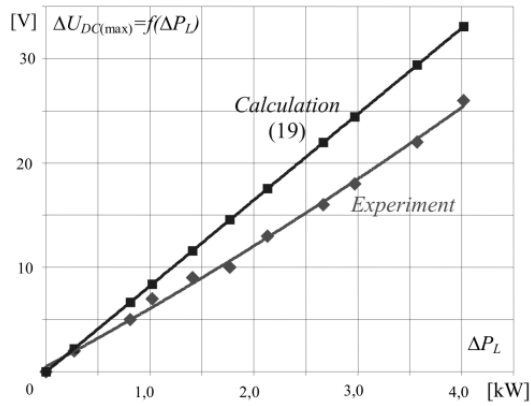


Fig. 10.  $\Delta U_{DC(max)}$  voltage deviations as a function of  $\Delta P_L$  increases

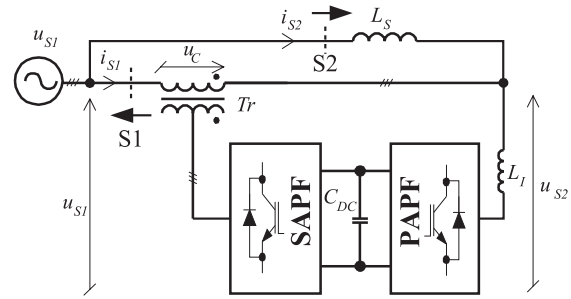


Fig.12. Connection scheme to investigate UPQC capabilities for power flow control.

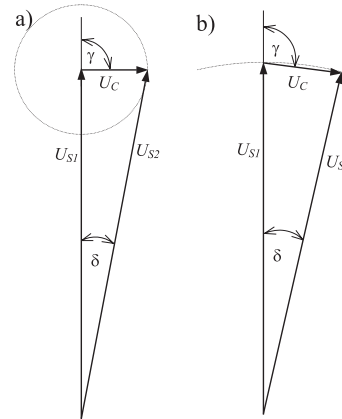


Fig. 13. Vector diagrams for verification power flow control methods

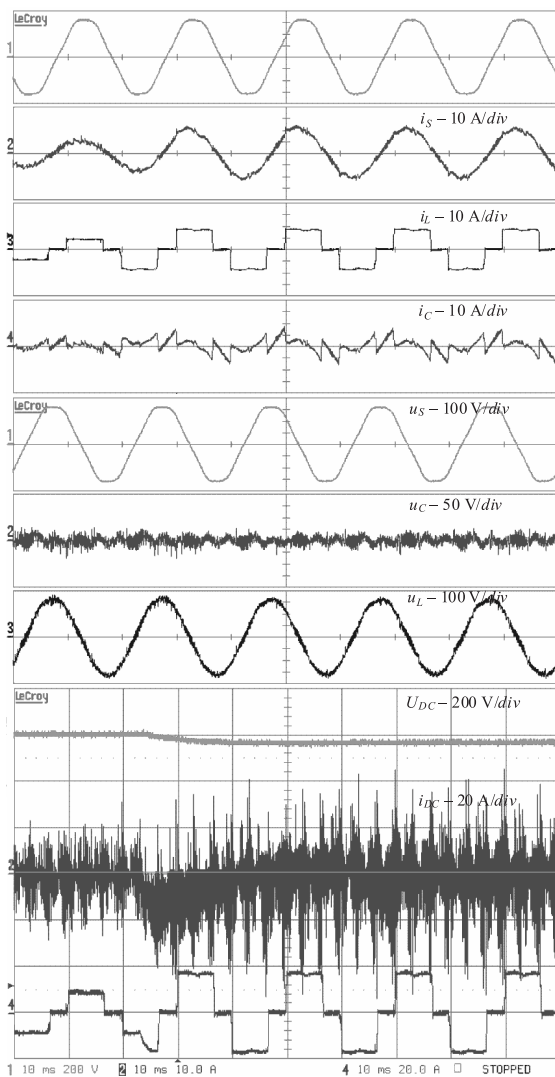


Fig.11. Experimental courses in situation of harmonics filtration and load step changes  $\Delta P_L$ , from 4kW to 8kW.

### 4.3. Additional functions—power flow control

UPQC with success can be used for power flow control. Considering the problem cognitively, a power flow controller generally can be represented as a synchronous voltage source (*SVS*), with frequency dependent on the network voltage frequency. An *SVS* should have the possibility of

control of its voltage: amplitude, in range  $0 \leq U_C \leq U_{Cmax}$ , and angle  $\gamma$  in limits:  $0 \leq \gamma \leq 2\pi$ . Figure 12 presents a connection scheme to investigate UPQC capabilities for power flow control. In UPQC, *SAPF* exchanges with transmission line active power (series active compensation) and reactive power (series reactive compensation), because of that there is possible power flow control. However, active power exchange, which mostly affects reactive power in the transmission line, is related to active power consumption from the *DC* link. Therefore *PAPF* in major part has to stabilize the  $U_{DC}$  voltage.

UPQC, behaving as power flow controller, can be controlled in accordance with two rules, presented in Figure 13. The vector diagram in Figure 13a. introduces a situation, when added voltage has constant amplitude  $U_C = const$ , and in this case only angle  $\gamma$  is changed in the range  $(0 \div 2\pi)$ . Such technique of control cases however, variable voltage load  $U_{S2}$ . If voltage  $U_{S2}$  has to be stabilized, UPQC should be controlled in accordance with the rule introduced in Figure 13b. In this case, there are changed: amplitude of the  $U_C$  adding voltage as well as  $\delta$  angle. In Figure 14 simulation and experimental voltage and current courses, for UPQC working in accordance with rule from Figure 13a, were introduced. As one can see, the experimental and simulation results agree, however such control causes changes in  $U_{S2}$  load voltage. Characteristics of changes of active and reactive power as a function of variable  $\gamma$  angle are presented in Figure 15. As one can see, characteristics confirm the UPQC power flow control capabilities.

In Figure 16 simulation and experimental voltage and current courses, for a UPQC arrangement working in

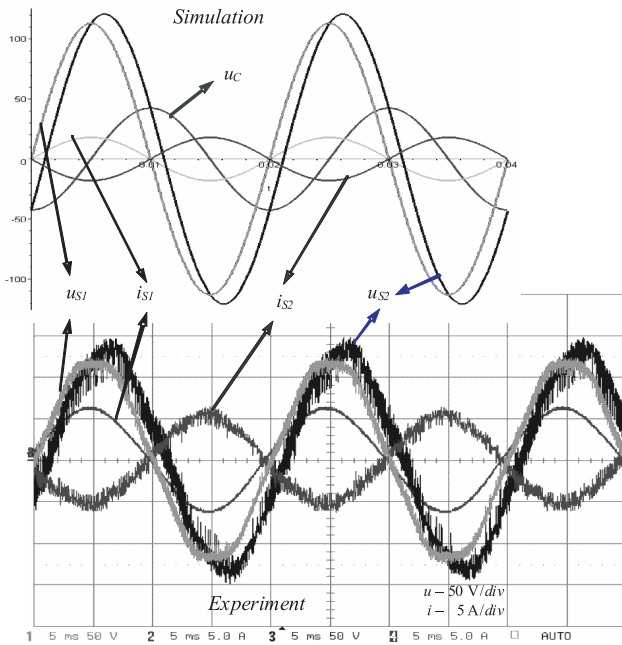


Fig.14. Simulation and experimental for 1<sup>st</sup> method as in Fig. 13a

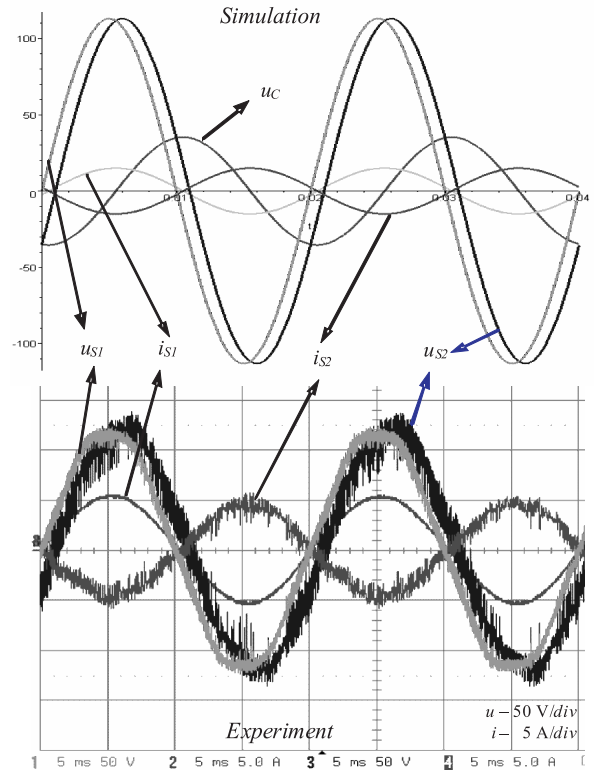


Fig.16. Simulation and experimental for 2<sup>nd</sup> method as in Fig.13b

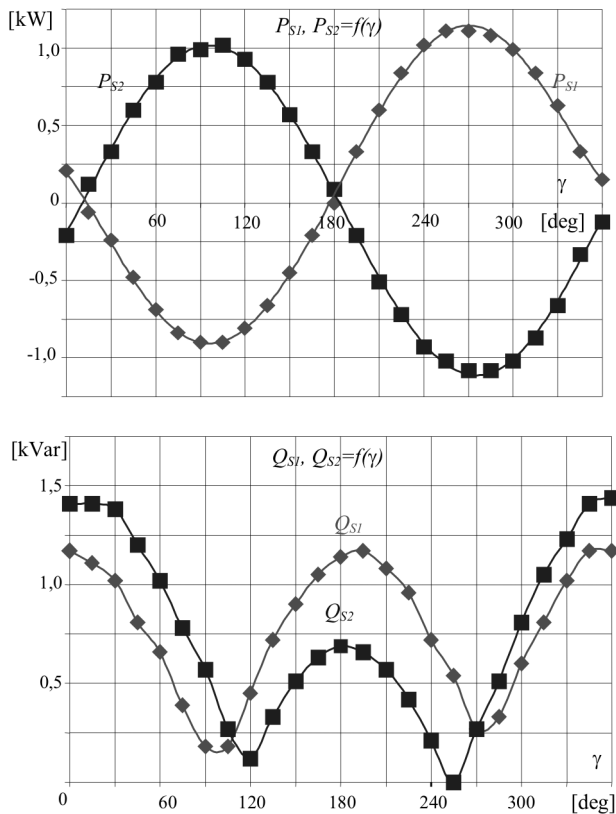


Fig.15. Active and reactive powers, measured at S1 and S2 points for 1<sup>st</sup> method

accordance with rule from Figure 13b, were introduced. As one can see experimental and simulation results are the same. Characteristics of changes of active and reactive power as a function of variable d angle are presented in Figure 17.

The second method of control is equivalent to the situation when SAPF exchanges with the transmission line mainly the reactive power (series reactive compensation). In

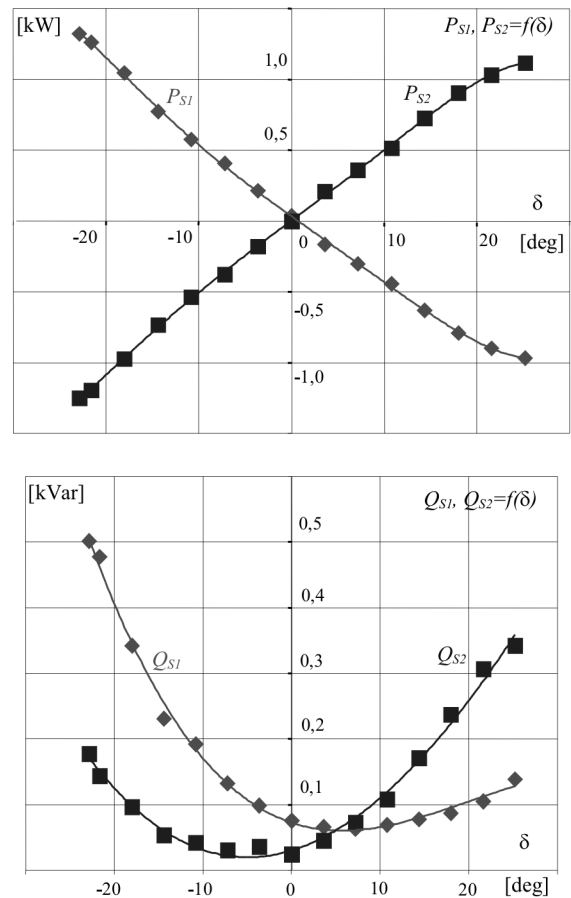


Fig.17. Active and reactive powers, measured at S1 and S2 points for 2<sup>nd</sup> method

consequence predominantly in the transmission line the active power is changed, range of reactive power control is smaller than in first case (Figure 13a).

## 5. CONCLUSIONS

In this paper method for analytic determination of *DC* link capacitor coupling both parallel and series arrangements, was worked out and verified experimentally.

Experimental investigations, including among others UPQC operation in situation of load with thyristor rectifier, were introduced. Results are confirming good compensating properties as well as multi-functionality of the UPQC. Investigated arrangement simultaneously permits to fulfill the following functions: voltage and current harmonics compensation, network voltage and load current symmetrization as well as network voltage stabilization and power flow control.

## REFERENCES

1. Akagi H.: *New trends in active filters*. Conf. Proc. EPE'95, 1995, s. 0.017–0.026.
2. Aredes M., Heumann K., Watanabe E.H.: *An Universal Active Power Line Conditioner*. IEEE Trans. on Power Delivery, Vol.13, No.2, 1998, pp.1453–1460.
3. Donghua Chen, Shaojun Xie: *Review of the control strategies applied to active power filters*. Proc. of the 2004 IEEE Int. Conf. on Electric Utility Deregulation, Restructuring and Power Technologies, 2004. (DRPT'2004). Vol.2, 2004, pp.666–670.
4. El-Habrouk M., Darwish M.K., Mehta P.: *Active power filters: a review*. IEE Proceedings- Electric Power Applications. Vol.147, No.5, 2000, pp. 403–413.
5. Fujita H. and Akagi H.: *Unified power quality conditioner: The integration of series and shunt active filter*. IEEE Trans. Power Electron., Vol. 13, No. 2, 1998, pp. 315–322.
6. Ghosh A., Ledwich G.: *A unified power quality conditioner (UPQC) for simultaneous voltage and current compensation*. Electric Power Systems Research, Vol. 59, 2001, pp. 55–63.
7. Malabika Basu M., Das S.P., Dubey G.K.: *Performance Study of UPQC-Q for Load Compensation and Voltage Sag Mitigation*. Proc. of the Conf. IECON'2002, 2002, pp. 698–702.
8. Strzelecki R.: *New concepts of the conditioning and power flow control in the AC distribution systems*. Proc. of the V Int. Conf. "Modern Feed Equipments in Electrical Power Systems", 2003, pp.65–72.
9. Strzelecki R. et. al.: *Modeling and experimental investigation of the small UPQC systems*. Proc. of the IV Conf. "Compatibility in Power Electronics – CPE'2005," Gdynia, 2005, CDROM, 15 p.
10. Watanabe E.H., Aredes, M.: *Power quality considerations on shunt/series current and voltage conditioners*. Proc. of the 10th Int. Conf. on Harmonics and Quality of Power, Vol.2, 2002, pp. 595–600.



### Grzegorz Benysek

was born in Sulechów, Poland, on June 17, 1968. He received his undergraduate education at the Technical University of Zielona Góra (M.S.E.E 1994, Ph.D. 1998). Now he is a postdoctoral fellow in Institute of Electrical Engineering at the University of Zielona Góra.

He has authored and co-authored about 70 journal and conference papers. His major research interest include analysis and control of power electronics circuits, control methods and properties investigations of the filtration systems like: active power filters, hybrid filters, series-parallel filters and also FACT devices. Additionally his researches are going in direction of utilization of the renewable energy sources in FACTS and custom power technologies.

Address:

Grzegorz Benysek

University of Zielona Góra

Institute of Electrical Engineering

50 Podgórna Str., 65-246 Zielona Góra, POLAND

phone:(+48 68) 3282417, fax:(+48 68) 3254615

e-mail: G.Benysek@iee.uz.zgora.pl